Journal of Hip Preservation Surgery Vol. 7, No. 4, pp. 748–754
doi: 10.1093/jhps/hnab024
Advance Access Publication 12 April 2021
Research article

OXFORD

3D-printed models for periacetabular osteotomy surgical planning

B. Keegan Markhardt [1,*], Matthew A. Beilfuss [2], Scott J. Hetzel [3], David C. Goodspeed [2] and Andrea M. Spiker [2]

[1]Department of Radiology, University of Wisconsin-Madison, University of Wisconsin Clinical Science Center, 600 Highland Ave. Madison, WI 53792, USA,
[2]Department of Orthopedic Surgery, University of Wisconsin-Madison, University of Wisconsin Clinical Science Center, 600 Highland Ave. Madison, WI 53792, USA and
[3]Department of Biostatistics and Medical Informatics, University of Wisconsin-Madison, University of Wisconsin Clinical Science Center, 600 Highland Ave. Madison, WI 53792, USA.
*Correspondence to: B. K. Markhardt. E-mail: keegan.markhardt@gmail.com
Submitted 22 June 2020; Revised 19 January 2021; revised version accepted 15 March 2021

ABSTRACT

The purpose of this study was to determine the feasibility and clinical benefits of using 3D-printed hemipelvis models for periacetabular osteotomy preoperative planning in the treatment of hip dysplasia. This retrospective study included 28 consecutive cases in 26 patients, with two bilateral cases, who underwent periacetabular osteotomy between January 2017 and February 2020 and had routine radiographs, CT and MR imaging. Of these, 14 cases [mean patient age 30.7 (SD 8.4) years, 11 female] had routine preoperative imaging, and 14 cases [mean patient age 28.0 (SD 8.7) years, 13 female] had routine preoperative imaging and creation of a full-scale 3D-printed hemipelvis model from the CT data. The expected surgical cuts were performed on the 3D-printed models. All patients underwent Bernese periacetabular osteotomy. Operative times, including time to achieve proper acetabular position and total periacetabular osteotomy time, fluoroscopy radiation dose and estimated total blood loss were compiled. ANOVA compared outcome variables between the two patient groups, controlling for possible confounders. On average, patients who had additional preoperative planning using the 3D-printed model had a 5.5-min reduction in time to achieve proper acetabular position and a 14.5-min reduction in total periacetabular osteotomy time; however, these changes were not statistically significant ($P = 0.526$ and 0.151, respectively). No significant difference was identified in fluoroscopy radiation dose or total blood loss. Detailed surgical planning for periacetabular osteotomy using 3D-printed models is feasible using widely available and affordable technology and shows promise to improve surgical efficiency.

INTRODUCTION

Developmental dysplasia of the hip includes a range of structural abnormalities of the acetabulum resulting in reduced coverage of the femoral head and varying degrees of joint instability. The incidence ranges between 0.06 and 76.1 per 1000 people, depending on ethnicity, with a 4–1 female predominance [1]. Hip dysplasia can produce debilitating pain and lead to early onset hip osteoarthritis [2].

Periacetabular osteotomy (PAO) is an effective joint-preserving surgical technique for restoring functional anatomy in hip dysplasia [3, 4] and has been shown to reverse the natural history of dysplasia-induced osteoarthritis [5]. During PAO, the bone around the acetabulum is cut and the fragment is rotated and secured into a new position to stabilize the joint [6, 7]. PAO is a technically challenging surgery performed under fluoroscopic guidance and requiring a detailed understanding of the patient's anatomy [8]. Preoperative radiographs, CT and MRI are routinely acquired for diagnosis and surgical planning [9].

3D printing is now a readily available and affordable technology. Current studies suggest that the accuracy and reproducibility of anatomic models printed with 3D printers are better than 1 mm and typically better than 0.5 mm, analogous to the spatial resolution of most clinical imaging modalities [10]. Using this technology, routine CT images can be used to make models of the skeletal system, which can be cut or drilled for operative simulation, depending on the material used for printing. Moreover, these models provide a tactile and visual experience useful in clinical diagnosis, surgical simulation, surgical planning, patient communication and medical education [11–13].

The use of 3D-printed models for PAO surgical planning has recently been described in two case series [14, 15]. In these investigations, preoperative simulation for PAO subjectively helped to assess the accuracy of the osteotomy line, determine the position of the osteotomized fragment, and prevent anterior impingement after the operation. The purpose of this project was to determine the feasibility and clinical benefits of using 3D-printed hemipelvis models for PAO surgical planning in a controlled study.

MATERIALS AND METHODS

This retrospective study was performed in compliance with Health Insurance Portability and Accountability Act regulations, with the approval of our Institutional Review Board, with a waiver of informed consent.

Study groups

A total of 28 consecutive patients with symptomatic hip dysplasia undergoing Bernese PAO surgery at our institution between January 2017 and February 2020 met inclusion criteria. PAO revision surgeries were excluded. All included patients were skeletally mature based on Risser stage of five. Starting November 2018, we began using a 3D model of the affected hemipelvis for preoperative planning. No other relevant changes were made to preoperative planning during this time period. There were 26 unique patients included. In our control group, we had 14 hip surgeries in 14 patients with routine preoperative planning (non-3D print group). In our study group, we had 14 hip surgeries in 13 patients who additionally had the creation of a 3D-printed model for preoperative planning (3D print group). One patient had bilateral surgeries with one surgery performed in each group, and one patient had bilateral surgeries in the study group. Patient age, gender and BMI, and affected hip laterality for each group are summarized in Table I.

Radiographic and CT examinations

No additional imaging was performed on the patients for this study. Routine preoperative and intra-operative radiographic views were obtained using digital radiography, including standing anteroposterior view of the pelvis and false-profile view of the affected hip. Lateral center-edge angle, anterior center-edge angle and the Tönnis angle [16] were measured at the time of the preoperative work-up by A.M.S., a board certified orthopedic surgeon with Hip Preservation fellowship training, and confirmed retrospectively by B.K.M., a board certified radiologist with musculoskeletal radiology fellowship training, with no discrepancy. The average preoperative measurements are summarized in Table I.

Hip CT was performed on all patients using the routine hip preservation protocol at our institution. This protocol consists of a CT of the pelvis from the iliac crest level to 6 cm below the lesser trochanter level and a CT of the knee from just superior to the epicondyle level to just inferior to the head of the fibula level. Acquisition parameters for the CT pelvis portion were: detector rows 32.0, kV 120, mA 200 with manual automatic exposure control, noise index 5.0, slice thickness 0.625 mm and slice interval 0.312 mm. Acquisition parameters for the CT knee portion were: detector rows 32.0, kV 120, mA 200, noise index 2.5, slice thickness 2.5 mm and slice interval 2.5 mm. The 3-mm bone window (2500WW/350WL) reformats were created in the axial, coronal and sagittal planes, and 2-mm bone window reformates were created in the axial oblique plane of the femoral neck. Coronal and sagittal center-edge angle using the sourcil margin [17], acetabular version at 1 o'clock, 2 o'clock and 3 o'clock, and femoral version [18] were retrospectively remeasured for consistency by B.K.M.

3D printing and preoperative surgical planning

The CT DICOM images were segmented using 3D Slicer (version 4.8.1) software (https://www.slicer.org) [19]. The editor function 'Level Tracing' was employed to segment the affected hemipelvis (innominate bone). Print preparation was made using Cura (version 4.5.0) software and fused deposition type 3D printing was made on an Ultimaker 3 printer (Ultimaker) using polylactic acid (PLA) filament (Ultimaker). The following parameters were used for printing: layer height 0.2 mm, wall thickness 2 mm, and, in order to print the model hollow, infill 0% and 'Mesh Fixes: Remove All Holes'. Hollow PLA models were easily cut with the oscillating bone saw with less debris to navigate than models with infill. The average print time was 15 h and 54 min, the average amount of filament used was 168 g, averaging $11.17 USD per model at $50 USD per 750-g roll of filament.

Prior to surgery, A.M.S. performed the expected PAO cuts on the 3D model using the same type of oscillating bone saw (Stryker) used for surgery. The cut acetabulum was rotated to the desired surgical position and fixed with hot melt adhesive for preoperative reference.

Table I. Patient demographics, radiographic and CT preoperative measurements reported as mean (standard deviation)

	Non-3D print group	*3D print group*	P-*value*
Number of cases	14	14	
Patient age	30.7 (8.4)	28.0 (8.7)	0.409
Gender—male: female	3:11	1:13	0.596
BMI	26.1 (4.4)	25.4 (4.0)	0.683
Laterality—right: left	9:5	9:5	1
Lateral center-edge angle[a]	13.8 (5.2)	12.3 (7.0)	0.525
Anterior center-edge angle	24.8 (11.5)	20.3 (11.5)	0.344
Tönnis angle	17.5 (4.5)	17.7 (7.0)	0.934
Coronal center-edge angle	15.9 (5.8)	12.5 (6.1)	0.151
Sagittal center-edge angle	44.6 (8.1)	41.0 (8.8)	0.27
Acetabular version at 1 o'clock	8.2 (8.9)	8.2 (6.5)	1
Acetabular version at 2 o'clock	14.7 (8.9)	15.6 (8.3)	0.788
Acetabular version at 3 o'clock	20.7 (7.3)	20.7 (7.5)	0.984
Femoral version	19.4 (15.1)	15.2 (10.9)	0.425

BMI, body mass index in kg/m^2.
[a]Angles are reported in degrees.

Surgery

All patients underwent Bernese PAO surgery performed by A.M.S., a board certified orthopedic surgeon with Hip Preservation fellowship training, and D.M., a board certified orthopedic surgeon with Trauma fellowship training, both with extensive experience in PAO surgery. Surgery was performed through an anterior approach utilizing a bikini incision. The acetabulum was mobilized through a series of cuts maintaining the continuity of the pelvic ring, including osteotomy of the anterior superior iliac spine, superior ramus, ischium, supra-acetabular iliac and, finally, posterior column [6, 7] with a rectus sparing approach. Meticulous care was taken to optimize the final position of the acetabulum. The goal was a femoral head that is medialized and well centered under a horizontal roof of the acetabulum. This was judged on AP and false-profile views taken with fluoroscopy and intra-operative AP pelvic radiographs. Care was taken to avoid uncovering the posterior aspect of the femoral head by overcorrecting anterior coverage or retroverting the acetabulum. The fragment was temporarily fixed in place for assessment with K-wires. Once final fragment position was achieved, it was secured with four screws (two anterior 3.5 mm and two posterior 4.5 mm cortical screws). Additional procedures were performed depending on the case, including concomitant hip arthroscopy with labral repair, cam decompression, subspine decompression and capsular closure. These additional surgeries were noted. There were no operative complications noted during the time of this study.

The following surgical data were collected: (i) total procedural time, defined as the time between the first incision and closure as documented in the operative note; (ii) total time of PAO, defined as the time between the first ischial cut and final screw fixation of the acetabulum as recorded by fluoroscopic spot image; (iii) time of ischial cut and (iv) time of posterior column cut, defined as the time between the beginning and completion of these cuts as recorded by fluoroscopic spot images; (v) time to proper acetabular position, defined as the time between completion of the posterior column cut, which marks the separation of the acetabulum from the pelvis, and the K-wire fixation as recorded by intra-operative radiograph; (vi) time to final fixation, defined as the time between the final posterior column cut and the final screw fixation as recorded by fluoroscopic spot image; (vii) time of anesthesia, defined as the time between the anesthesia start and stop time as per the anesthesia record; (viii) estimated total blood loss in milliliters from the surgical record; (ix) total fluoroscopy time in minutes, and (x) radiation dosage in milligray from the fluoroscopy device record.

Statistical analysis

Demographic variables were summarized by 3D print and non-3D print cases with mean or number based on statistical distribution. Two-sample *t*-tests or Fisher's exact tests were used to evaluate for confounding differences between the groups with regards to the degree of disease as indicated by preoperative radiographic and CT measurements. Intra-op times were compared between 3D print and non-3D print groups using ANOVA models controlling for age at surgery, gender and BMI. Total surgical time, estimated total blood loss and total fluoroscopy radiation dose were compared between the groups using ANOVA models that additionally controlled for the presence or absence of concurrent arthroscopic surgeries. One patient had bilateral surgeries with one surgery in each group, and one patient had bilateral surgeries in the 3D-printed study group. With only two subjects with repeated measures and the likelihood that subsequent bilateral surgical times are independent of the initial surgical times, data were analyzed as independent samples. Analysis was conducted in R for statistical computing version 3.53 [20]. Statistical significance was set at a *P*-values <0.05.

RESULTS

3D models were successfully printed for patients in the 3D-print group before surgery, and the expected PAO surgical cuts were made on the models, as illustrated in Fig. 1. There were no inaccuracies between the models and the CT scans by visual inspection. There were no significant differences in patient demographics or acetabular measurements between the preoperative 3D-print group and the non-3D print group, as summarized in Table I. No significant differences were identified between the various surgical times, controlling for age, gender and BMI, as summarized in Table II. While not significant, the mean time to achieve proper acetabular position was 5.5 min shorter and the mean total PAO time was 14.5 min shorter in the 3D print group. No significant differences were identified in fluoroscopy time, fluoroscopy radiation dose, total procedure time, total anesthesia time or total blood loss between the groups, controlling for age, gender, BMI and concurrent arthroscopic procedures, as summarized in Table II.

DISCUSSION

We found it was feasible to 3D print a model of a patient's hemipelvis using the CT scan routinely obtained for PAO operative planning, open-source software and widely available 3D-printing technology. The expected PAO surgical cuts were successfully performed on the 3D-printed models using an oscillating bone saw and the cut acetabular fragment could be rotated and fixed into the expected final operative position for reference. While our study failed to show any statistically significant evidence of improved surgical efficiency, use of the models subjectively improved our understanding of patient-specific bony anatomy. We observed reductions in the operative times, including mean time to achieve the proper acetabular position and the mean total PAO time, and therefore this technique shows promise to improve surgical efficiency.

To our knowledge, three studies have explored the utility of 3D model printing in PAO planning. Fukushima *et al.* [15] developed a method for simulating PAO on an anatomically correct 3D-printed salt model. While promising, the method of salt model creation that they employed

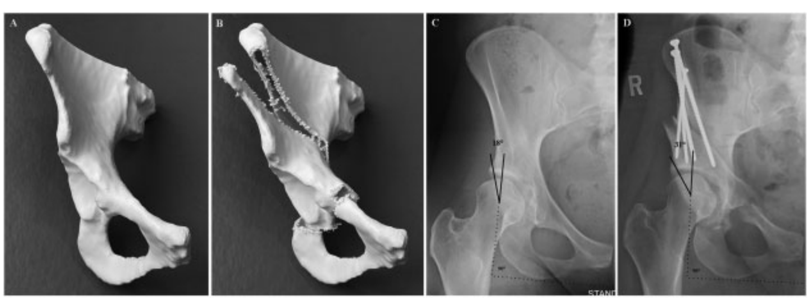

Fig. 1. A 29-year-old woman with right hip dysplasia undergoing evaluation and PAO. Photographs of the 3D-printed model hemipelvis taken before (**A**) and after (**B**) expected PAO cuts (and glue fixation) for preoperative planning. Preoperative (**C**) and postoperative (**D**) standing anteroposterior pelvis radiographs show treatment of the dysplastic acetabulum with the lateral central edge angle measuring 18° before surgery and 31° after surgery.

Table II. Surgical times, fluoroscopy dose and time, anesthesia time and estimated blood loss reported as mean (standard deviation)

	Non-3D print group	*3D print group*	*Univariable P-value*	*Multivariable P-value*
Total time of PAO[a] (min)	132.9 (30.3)	118.4 (20.3)	0.151	0.089[b]
Ischial cut time (min)	11.9 (6.3)	12.4 (7.1)	0.833	0.95[b]
Posterior column cut time (min)	14.4 (9.8)	12.7 (7.6)	0.641	0.472[b]
Time to proper acetabular position (min)	54.9 (25.5)	49.4 (17.6)	0.526	0.257[b]
Time to final fixation (min)	91.2 (26.9)	79.5 (19.9)	0.212	0.084[b]
Fluoroscopy time (min)	2.6 (0.5)	2.7 (0.6)	0.829	0.879[c]
Fluoroscopy dose in mGy	69.8 (22.8)	65.0 (26.7)	0.619	0.731[c]
Total procedure time (min)[d]	387.9 (60.6)	380.8 (60.7)	0.757	0.849[c]
Total anesthesia time (min)[d]	465.3 (63.3)	455.3 (63.2)	0.678	0.920[c]
Estimated total blood loss in ml	850.4 (479.9)	586.1 (274.3)	0.088	0.315[c]

PAO, periacetabular osteotomy; mGy, milligray; ml, milliliter.
[a]Times are in minutes and time periods are described in the text.
[b]Controlling for age, gender and BMI.
[c]Controlling for age, gender, BMI and concurrent arthroscopic procedures.
[d]These procedures all included concomitant hip arthroscopy, with separate prepping/draping for the hip arthroscopy, closure and dressing after hip arthroscopy, moving the patient to a separate table for PAO, re-prepping and re-draping for the PAO, which explains the duration of total procedure as being much longer than the total PAO time.

is not widely available and currently requires expertise in model making. A case study by Holt *et al.* [14] highlighted the importance of hands-on surgical planning in improving surgical precision, which we found to be subjectively true. Finally, recent case series by Bockhorn *et al.* [21] added 3D models to PAO preoperative planning for a series of 16 patients and surveyed hip preservation surgeons, orthopedic trainees and patients. Patients and trainees believed that the prototypes enhanced their educational experience, noting that the surgeon could directly demonstrate complex morphological abnormalities. Surgeons also believed that the models improved trainee and patient education, especially in cases of atypical pathomorphology. Our experience is consistent with the authors' findings, and we believe that the models provided an unparalleled educational opportunity about the PAO procedure to our trainees in orthopedic surgery and radiology, as well as the operating room staff, including surgical technologists, nurses and anesthesiology staff.

A number of studies have looked at various uses of 3D-printed models for surgical planning [11, 12, 22, 23]. For example, Wong *et al.* [23] found 3D models to be helpful for the treatment of femoroacetabular impingent. Specifically, the authors found that evaluation of the model before surgery changed both the extent and location of the planned osteoplasty. In a recent case series of patients with 3D-printed anatomy undergoing spine, skull, hip, foot and knee surgeries, Galvez *et al.* [22] found a decrease in surgical time, a decrease in blood loss and a reduction in the amount of anesthesia. The authors also noted improved anatomic information that resulted in changes to surgical strategy in two cases. These findings are supported by two recent systematic reviews have been made on a growing body of literature exploring the use of 3D printing in medicine. In a systematic review of 227 surgical studies describing the use of 3D printing for surgical guides, anatomic models and custom implants, Tack *et al.* [11] identified reduced surgical time, improved medical outcome and decreased radiation exposure as major advantages to the technique. In systematic review of 158 studies on medical molds, implants, surgical guides and anatomic models created using 3D printers, Martelli *et al.* [12] found that the greatest benefits were reported in preoperative planning and the time saved in the operating room.

Systematic reviews have identified a need for cost analysis when considering this technology, especially when used for creation of implantable devices and surgical guides where higher-end manufacturing techniques and expertise in industrial design are needed [11, 12]. In the 2018, the American Medical Association adopted a group of Category III codes for 3D anatomic modeling to qualify and observe this emerging technology; however, billable codes have not been determined at this time. Our cost for anatomic model creation was low, with low material costs, open-source software and uncompensated physician time. To operationalize 3D-printing services at a health center compensated physician, technician or scientist time would be appropriate, and, in the United States, FDA approved software is required [24], which adds the cost of licensing fees.

The primary limitation of this study was that the non-3D print and 3D print group were sequential and not randomized, raising the possibility that any improvement in surgical efficiency could be attributed to increasing surgical experience and not the use of the 3D print. If we had statistically significant results, then we would have evaluated for this confounding factor by evaluating for in-group trends in surgical efficiency. Second, because there is a wide range of hip dysplasia morphology, small group sizes might be affected by differences in the degree of disease between the groups. We assessed for differences between the groups using the CT and radiographic measurements of dysplasia and found no clear confounding differences. Third, total operative time, anesthesia time, total blood loss and total radiation dose measures were influenced by additional surgical procedures at the time of PAO surgery, including arthroscopic cam decompression, subspine decompression, labral repair and capsular closure. We attempted to control for the presence or absence of these elements, but likely they affected our measures in ways that cannot be controlled for due to variation in the surgical demands of each element. Finally, we did not assess for the accuracy of the 3D models. One of the largest sources of inaccuracy in 3D model creation from medical imaging is the step of segmenting the target tissue, which is often related to using automated methods, such as threshold-based segmentation [10]. Threshold-based segmentation proved inaccurate with our software and CT imaging technique; therefore, we used the semi-automated method of 'Level Tracing' each CT image slice to more faithfully segment the target bone. To evaluate model accuracy, we could have CT scanned the models for direct comparison with the patient CT scan; however, for this application, there were no perceivable disparities, and this degree of accuracy was not thought to be required.

Further research is needed to determine how well the planned correction on the model was achieved at surgery, and whether radiographing the treated model could be helpful for operative reference. We radiographed the model hemipelvis and attempted to make correction and cut angle measurements; however, the radiographic views and measurements proved to be arbitrary without the full pelvis and affected femoral head for guidance, and therefore were not included in this study. From our experience, in order to translate the desired correction into the intra-operative situation, radiographic imaging and measurements of a treated full pelvis model would be needed.

CONCLUSION

Detailed surgical planning using 3D printing for PAO is feasible using widely available and affordable technology. The technique shows promise to improve surgical efficiency and was subjectively helpful in understanding the unique patient-specific anatomy of the pelvis and in educating surgical trainees.

CONFLICT OF INTEREST STATEMENT

None declared.

FUNDING

Research support for M.A.B. was provided by an award from the University of Wisconsin School of Medicine and Public Health and the Herman and Gwendolyn Shapiro Foundation.

DATA AVAILABILITY STATEMENT

The data underlying this article will be shared on reasonable request to the corresponding author.

REFERENCES

1. Loder RT, Skopelja EN. The epidemiology and demographics of hip dysplasia. *ISRN Orthopedics* 2011; **2011**: 238607.
2. Pun S. Hip dysplasia in the young adult caused by residual childhood and adolescent-onset dysplasia. *Curr Rev Musculoskelet Med* 2016; **9**: 427–34.
3. Leunig M, Siebenrock KA, Ganz R. Rationale of periacetabular osteotomy and background work. *Instr Course Lect* 2001; **50**: 229–38.
4. Villar R. What is hip preservation? *J Hip Preserv Surg* 2018; **5**: 103–4.
5. Wyles CC, Vargas JS, Heidenreich MJ *et al.* Natural history of the dysplastic hip following modern periacetabular osteotomy. *J Bone Joint Surg Am* 2019; **101**: 932–8.
6. Ganz R, Klaue K, Vinh TS, Mast JW. A new periacetabular osteotomy for the treatment of hip dysplasias. Technique and preliminary results. *Clin Orthop Relat Res* 1988; **232**: 26–36.

7. Malta JM, Stover MD, Siebenrock K. Periacetabular osteotomy through the Smith-Petersen approach. *Clin Orthop Relat Res* 1999; **363**: 21–32.
8. Novais EN, Carry PM, Kestel LA *et al.* Does surgeon experience impact the risk of complications after Bernese periacetabular osteotomy? *Clin Orthop Relat Res* 2017; **475**: 1110–7.
9. Albers CE, Rogers P, Wambeek N *et al.* Preoperative planning for redirective, periacetabular osteotomies. *J Hip Preserv Surg* 2017; **4**: 276–88.
10. George E, Liacouras P, Rybicki FJ, Mitsouras D. Measuring and establishing the accuracy and reproducibility of 3D printed medical models. *Radiographics* 2017; **37**: 1424–50.
11. Tack P, Victor J, Gemmel P, Annemans L. 3D-printing techniques in a medical setting: a systematic literature review. *Biomed Eng Online* 2016; **15**: 115.
12. Martelli N, Serrano C, van den Brink H *et al.* Advantages and disadvantages of 3-dimensional printing in surgery: a systematic review. *Surgery* 2016; **159**: 1485–1500.
13. Starosolski ZA, Kan JH, Rosenfeld SD *et al.* Application of 3-D printing (rapid prototyping) for creating physical models of pediatric orthopedic disorders. *Pediatr Radiol* 2014; **44**: 216–21.
14. Holt AM, Starosolski Z, Kan JH, Rosenfeld SB. Rapid prototyping 3D model in treatment of pediatric hip dysplasia: a case report. *Iowa Orthop J* 2017; **37**: 157–62.
15. Fukushima K, Takahira N, Uchiyama K *et al.* Pre-operative simulation of periacetabular osteotomy via a three-dimensional model constructed from salt. *Sicot J* 2017; **3**: 14.
16. Clohisy JC, Carlisle JC, Beaulé PE *et al.* A systematic approach to the plain radiographic evaluation of the young adult hip. *J Bone Joint Surg Am* 2008; **90**(Suppl. 4): 47–66.
17. Wylie JD, Kapron AL, Peters CL *et al.* Relationship between the lateral center-edge angle and 3-dimensional acetabular coverage. *Orthop J Sports Med* 2017; **5**: 2325967117700589.
18. Kang RW, Park C, Ranawat A. *Computer Tomography Scan of the Hip and Pelvis*. New York, NY: Springer, 2015, 53–63.
19. Kikinis R, Pieper S, Vosburgh K. 3D Slicer: a platform for subject-specific image analysis, visualization, and clinical support. In: Jolesz FA (ed). *Intraoperative Imaging Image-Guided Therapy*, vol. 3. 2014, 277–89.
20. Team RC. *R: A Language and Environment for Statistical Computing*. Vienna, Austria: R Foundation for Statistical Computing, 2014.
21. Bockhorn L, Gardner SS, Dong D *et al.* Application of three-dimensional printing for pre-operative planning in hip preservation surgery. *J Hip Preserv Surg* 2019; **6**: 164–9.
22. Galvez M, Asahi T, Baar A *et al.* Use of three-dimensional printing in orthopaedic surgical planning. *J Am Acad Orthop Surg Glob Res Rev* 2018; **2**: e071.
23. Wong TT, Lynch TS, Popkin CA, Kazam JK. Preoperative use of a 3D printed model for femoroacetabular impingement surgery and its effect on planned osteoplasty. *Am J Roentgenol* 2018; **211**: W116–21.
24. Kiarashi N. FDA Current Practices and Regulations. FDA/CDRH–RSNA SIG Joint Meeting on 3D Printed Patient-Specific Anatomic Models: FDA, 2017.